ACTA ACUSTICA UNITED WITH ACUSTICA
Vol. 94 (2008) 676 – 684

DOI 10.3813/AAA.918081

Scaled Laboratory Experiments of Shallow Water Acoustic Propagation: Calibration Phase

Panagiotis Papadakis, Michael Taroudakis*
FORTH/IACM, P.O. Box 1385, 711 10 Heraklion, Crete, Greece. panos@iacm.forth.gr, taroud@iacm.forth.gr

Frédéric Sturm
Laboratoire de Mécanique des Fluides et d'Acoustique, UMR CNRS 5509, Ecole Centrale de Lyon, 36, avenue Guy de Collongue, 69134 Ecully Cedex, France. frederic.sturm@ec-lyon.fr

Patrick Sanchez, Jean-Pierre Sessarego
Laboratoire de Mécanique et d'Acoustique, UPR CNRS 7051, 31 Chemin Joseph Aiguier, 13402 Marseille Cedex 20, France. sanchez@univ-cezanne.fr, sessarego@lma.cnrs-mrs.fr

Summary
Laboratory experiments in underwater acoustics aim at the validation of theoretical acoustic propagation models in well controlled environments. The experimental tank of the LMA Laboratory provides an ideal environment for testing long range propagation codes. The tank is relatively long and the water depth is adjustable in order to simulate real propagation experiments in environments of variable depths. The purpose of this paper is to describe the experimental procedure for the realization of a long range propagation experiment in an experimental tank, using sources of appropriate frequency. The bottom of the tank was covered by a thick layer of fine sand with well known properties to simulate a real.stic sea-bed. It was supposed to be horizontal and perfectly flat without any ripples on the surface. The measured, monochromatic continuous wave, signals are processed to provide the acoustic field at various depths and ranges in the tank in decibels, and are compared with theoretical models based on normal-mode theory and parabolic equations. The comparison in the cases studied, which corresponded to shallow water transmissions are encouraging. Technological problems and scaling factors are also discussed.

PACS no. 43.30.Zk

1. Introduction

Laboratory experiments for testing theoretical models of long-range acoustic propagation in the ocean are not easy to perform, in comparison with experiments aiming at the study of local reflectivity phenomena. This is mainly due to the fact that the simulation of a long range environment in a reduced scale, should be done with great care to ensure that the geometry of the experiment corresponds to the theoretical considerations especially in what concerns bottom horizontality and flatness, precise determination of water depth as well as precise location of both source and receiver. Most of the models predicting the sound field at long ranges in water are based on an axially symmetric environment. Thus, an experiment performed in a tank should ensure that no unwanted reflections from the walls could affect the measurements. To this end, not only wide and long tanks should be available, but also absorbing materials should be placed along the tank walls to avoid any spurious echoes. On the other hand, the structure simulating the bottom should be such that any assumptions adopted in the computer code should be well represented in the tank. Moreover, accurate calibration is needed as the experiments represent real-world experiments in scale. As the sound field in the sea is highly variable, even small errors in the geometry considered in the water tank or the operational parameters used in the computer code, may lead in high discrepancies between measured and estimated data, thus rendering validation of methods not possible.

Another difficulty when performing tank experiments is the scaling factor relating tank to real experiment, which cannot be applied to all of the parameters of the tank experiment (in particular attenuation cannot be scaled with the same scaling factor). Thus a one-to-one correspondence cannot be obtained. In addition, the validation of acoustic propagation models is still possible as the theoretical model can be applied in any case to the actual parameters of the tank experiment.

Tank experiments for underwater long-range propagation simulation have been performed successfully in the past [1]–[12] illustrating the fact that an experimental procedure in a tank, if carefully designed, is capable of pro-

Received 22 December 2006,
accepted 18 June 2008.

* also Department of Mathematics, University of Crete 71409 Heraklion, Crete, Greece

viding data for the validation of the acoustic propagation codes.

The objective of the work performed here is to provide a follow-up to the experiments described in [11, 12], using another tank facility of the same laboratory and different source/receiver instrumentation taken from the "shelf". The reason for insisting in performing systematic tests in tanks is the following: The standardization of the experimental procedures is essential if a facility is to be used for conducting experiments of different type at different times. It is also very important for the operators to be able to use alternative types of instruments, not necessarily designed for a specific type of experiments.

The specific tank at LMA was chosen as the site of experiments concerning inverse problems in underwater acoustics in 3-D environments. As it is well known that complicated geometries are difficult to be handled by theoretical models, it is well understood that any attempt to compare theoretical with measured data, should be based on careful analysis of the performance of the experimental facility in connection with the specific parameters controlling the reliability of the 3-D propagation models. To this end, the calibration of the tank facility is essential for the success of the whole procedure.

The calibration is performed using simple propagation geometries. Acoustic propagation problems in range-independent axially symmetric environments are well studied and numerous codes based on wave theory have been developed, all being able to provide accurate results in realistic low frequency propagation problems. Thus, there is no need for validating these codes using tank experiments. Instead, it is these codes that can be treated as the basis of the calibration of an experimental procedure. By tuning the unknown parameters of the experiment in such a way so as the measurements are well compared with the theoretical predictions under different conditions and geometries, always within the limits of applicability of the forward propagation models, the tank is considered ready to be used for the performance of scaled tank experiments under more complicated geometries and conditions.

The aim of the present paper is to describe and analyze the tank calibration process, which was considered necessary before starting the experiments in 3-D environments for the study of inverse problems in underwater acoustics. As it was expected that 3-D inverse modeling would be based on specific Parabolic approximation codes (PE codes), it was decided that the theoretical predictions should also be based on these codes. Thus, it was decided to calibrate the experimental procedure using both Normal-Mode and PE based numerical codes.

The final aim of the work which started with the procedures described here, is to define standards for the conduction of tank experiments aiming at the validation of long-range forward and inverse propagation models and the analysis of experimental procedures to be adopted in full scale under general geometrical and propagation conditions. It should be noted that some preliminary results of this work have been reported at conferences [13, 12, 14].

Figure 1. The experimental facility.

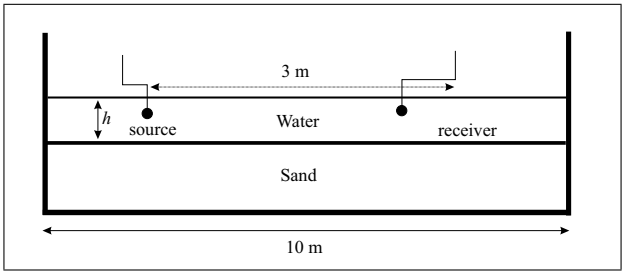

Figure 2. The experimental set-up (not to scale).

The structure of the paper is as follows: Next section is devoted to the description of the experimental facilities and instrumentation. It includes details of the calibration procedures, which were necessary in order to achieve the best possible accuracy of the geometry and the operational parameters of the experiments. Section 3 contains a brief analysis of the normal-mode and PE theoretical models applied for the comparison between theory and experimental data. In section 4, two of the test cases studied are presented and the procedure to achieve the best possible agreement between theory and experiment is discussed.

2. Experimental set-up

2.1. The facilities and the instrumentation

The experiments presented here were realized in the facilities of the LMA in Marseille. The tank used is 20 meters long, 3 meters wide and 1 m in depth (Figure 1). A portion of only 10 m was used for this experiment (Figure 2). Water can be poured up to a specified height to simulate a water column in the ocean of different depth. For the needs of the experiments performed, the actual water column height h was varying from about 40 to 70 mm between tests by pouring additional amount of fresh water that was carefully previously degassed. Wedge shaped absorbing materials have been used to avoid reflections from the walls of the tank.

To simulate the ocean bottom, a layer of sand was deposited at the floor of the tank. Its thickness was 40 cm. The sediment lying on the tank bottom was a calibrated sand whose granulometry can be seen on the Figure 3 (this curve was obtained with the Mastersizer 2000 from

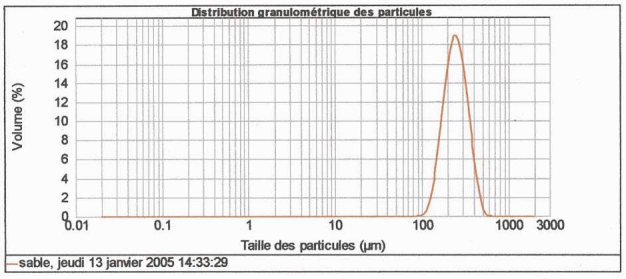

Figure 3. Distribution of the grain size of the sand.

Figure 4. The transducer.

Malvern Instruments). The size distribution was a gaussian function centered on the value 245 microns. The sand has been put in the tank long time ago and carefully degassed in order to avoid the presence of bubbles.

The experimental setup is depicted in Figure 2. Two cylindrically shaped hydrophones were used as source and receiver. The transducers were made in the laboratory. They are made of small piezoelectric hollow cylinders (diameter: 4 mm, height: 6 mm) coated with a polyurethane resin (see Figure 4). With this coating, the overall dimension of the source and receiver is 6 mm × 8 mm.

The tank is equipped with a system of mechanical beams moving on rails. Adjustable arms were attached on these beams, capable of carrying transducers and additional equipment. The whole system was computer controlled, thus giving great flexibility in changing the configuration of the experiments. During the experiment the receiver could be moved in the x, y and z directions by the use of stepping motors driven by a computer. The transmitter could be moved in an automatic mode only for z axis (depth). The received analog signal was immediately converted to digital by a sampling device installed in a computer placed on the moving carriage. The digital signals were then sent to the main computer by a high speed network.

2.2. Calibration

Initial measurements were carried out in order to specify the geometrical and physical parameters of the experiment. In particular the following parameters or properties were measured or controlled:

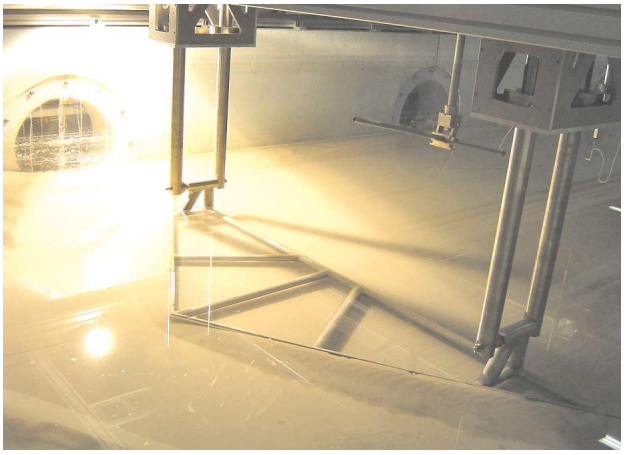

Figure 5. The rake.

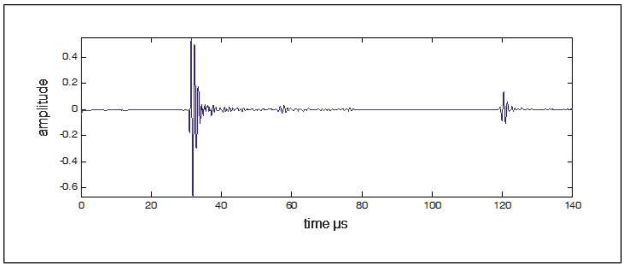

Figure 6. Measurement of the water depth: First signal corresponds to reflection from the bottom and the second strong signal corresponds to reflections from the bottom (twice) and the surface.

- *The flatness of the sand surface.* Particular care was taken to make the bottom as flat as possible. A special device (rake) was constructed, attached to the rails and was dragged along the length of the tank to ensure the flatness of the modeled water-bottom interface (Figure 5). Measuring the bathymetry the day before the experiment revealed that the anomalies of the bottom flatness were of the order of less than 0.1% of the water depth.
- *Water depth.* Using a high frequency transducer (at 5 MHz) placed in the water column at an arbitrary position, the depth of the water column was measured using travel time measurements of a signal transmitted vertically. Reflections from both the bottom and the surface were used (see Figure 6). The time was measured in ţsec. The sound speed used for the conversion of the time to distance was calculated (using the empirical formula suggested in [15]) on the basis of the water temperature which was continuously monitored and measured during the experiments. With this acoustical measurement the water depth could be estimated with a precision of 0.5 mm.
- *The operating depth of both source and receiver.* The position in depth of both transducers was determined electronically by means of the control device of the

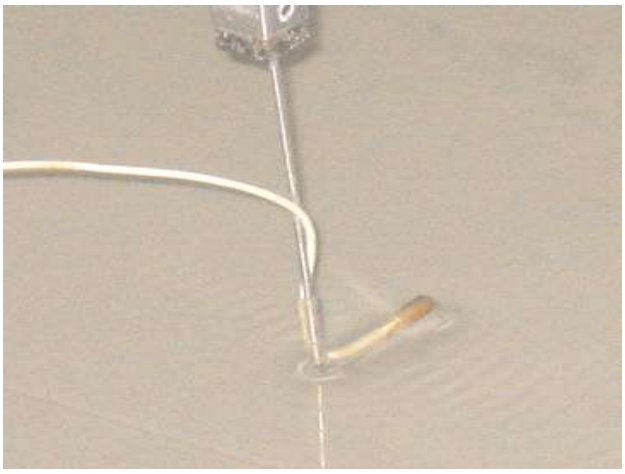

Figure 7. Confirming the zero depth level.

tank moving system, after determination of the zero (0) depth which was done using the following procedure: The transducer was put at certain depth and then it was slowly raised until the transducer was exactly at the surface. This position corresponds to the actual 0 of the depth position. The contact with the surface was difficult to be observed with naked eye or any other direct observation method, so a zoomed picture of the instrument from a digital camera was used as in Figure 7. This procedure ensures that relative positions of source and receiver are determined with acceptable accuracy; The error coming from the tensile strength of the water was not so important. Different measurements have shown that this error was of the order of ±0.5 mm. In addition the acoustic center of the transducer can differ from the geometrical center with less than 1 mm. In any case it is evident that a more elaborate procedure is needed in order to obtain the absolute position of source and receiver with the maximum possible accuracy.

- *Bottom geoacoustic parameters.* The bottom was made of sand, which has been put in the tank and degassed for a long time. Once the flattening of the surface was done, it was decided to wait for a few additional days before starting the experiment in order to ensure that good consolidation has been obtained. The compressional velocity in the sediment was measured using samples of the sand in the laboratory. Its value was found to be around 1700 m/s (±50 m/s). This measurement will be discussed in details in section 4. The density of the sediment was measured to be 1990 kg/m (±10 kg/m) The attenuation could not be measured but a typical value for the specific type of sediment was used.
- *The reference signal.* In order to be able to compare experimental data with theoretical results, we adopted the representation of the acoustic field using the notion of the transmission loss (TL). Thus a reference distance had to be considered in which measurements of the acoustic field should have been recorded (reference level). The experimental data presented herewith are referred to a reference distance of 1 cm. Prior to the realization of each experiment, the acoustic field due to the corresponding source was measured at that distance.

2.3. The experimental procedure

The design of the experiment was such that a 1:1000 scale factor was anticipated. Recall that the principle of scaled experiments is that the ratio of a characteristic dimension (e.g. the water depth) by the acoustic wavelength is invariant during the scaling, leading to the equality $h/\lambda = H/\Lambda$, where h and λ (respectively H and Λ) denote the water depth and the acoustic wavelength before (resp. after) the scaling. For instance, taking into account that the frequency of the signal of the first test was 104 kHz, the corresponding real experiment was associated with a source of 104 Hz. Note that the frequency of 104 kHz is considered "low" for tank experiments due to the fact that it is very difficult to manufacture very small transducers working at low frequencies. The frequency of the simulated experiment is also considered "low" for practical applications of underwater acoustics technology. It is however reasonable for applications of ocean acoustic tomography the simulation of which is one of the purposes of the experiments to be held later in this tank. As it is our purpose to simulate coastal zone tomography, a shallow water environment was to be considered. In order to simulate a shallow water experiment, the depth of the water column in the tank was decided to be of the order of 4-7 cm so that a real water depth from 40 m up to 70 m is considered. The maximum range used in the tank was about 3.0 m to simulate a real range of up to 3000 m, a typical configuration for a shallow water tomographic experiment.

3. The theoretical models

For the purpose of comparing theoretical and experimental results, numerical codes based on normal mode theory and the parabolic approximation have been used. The following paragraphs present a brief outline of the theory upon which the codes have been based.

3.1. Normal-mode theory

For the comparison of the measured acoustic field with theoretical predictions based on a normal mode representation of the acoustic field, the code MODE4 [16] has been used in its version for range-independent axially symmetric environments. The code treats fluid bottoms only. Assuming a cylindrical coordinate system with z being the depth below the ocean surface, and r the horizontal range from the source, the pressure field is given by the following expression:

$$p(r, z) = \sum_{n=1}^{N} A_n H_0^{(1)}(\kappa_n r)\, u_n(z)\, u_n(z_0), \qquad (1)$$

where $p(r, z)$ is the acoustic pressure, $u_n(z)$ is the eigenfunction of order n, κ_n is the associated eigenvalue, z_0 is the source depth, A_n is the normalization constant, $H_0^{(1)}$ is

the Hankel function of zero order and first kind, N is the maximum number of modes considered in the sum.

In our case, we have used an environment consisting of a single water layer of constant speed over a fluid half-space bottom. For this environment, the eigenfunctions satisfy the following boundary value problem,

$$\begin{aligned} &\frac{\partial^2 u_n}{\partial z^2}(z) + \left(k^2(z) - \kappa_n^2\right) u_n(z) = 0, \\ &u_n(0) = 0, \qquad u_n(h^-) = u_n(h^+), \\ &\frac{1}{\rho_w}\frac{\partial u_n}{\partial z}(h^-) = \frac{1}{\rho_b}\frac{\partial u_n}{\partial z}(h^+), \end{aligned} \tag{2}$$

where $k(z)$ is the wave number. It is constant in each of the two layers: $k(z) = \omega/c_w$ in the water and $k(z) = \omega/c_b$ in the bottom, with $\omega = 2\pi f$ and f the frequency in Hz. The parameter h is the water depth and ρ_w, ρ_b are the density in the water and in the bottom respectively.

For this case we know that the spectrum of the eigenvalues consists of a discrete plus a continuous spectrum [17]. For the theoretical calculations presented in this work, the continuous part is neglected, thus keeping in the sum the propagating modes only. This is known to be a very good approximation for long-range propagation cases. The computer code provides the Transmission Loss (TL) as a function of range and depth for a specified number of frequencies,

$$\mathrm{TL} = -20 \log \frac{\left| p(r, z) \right|}{\left| p_{\mathrm{ref}} \right|}, \tag{3}$$

where p_{ref} is a reference pressure, which by definition is considered as the acoustic pressure due to a point source in an unbounded domain (spherical spreading) at a specific distance. The TL calculated by the propagation codes is traditionally referred to a distance of one meter from the sound source. Taking into account that as stated before, reliable measurements of the acoustic field can be performed in the tank at a distance of no less than 1cm from the source transducer, the measured values of the TL should be referred to that distance.

It should be noted that attenuation in the bottom for a signal of high frequency as the one used in the experiment is very high, thus ensuring that practically no reflections from the actual tank bottom is expected. In fact Figure 6 shows that there is a very low reflection from the tank bottom which is more than 20 dB lower than the one from the water sand interface. Therefore the treatment of the seabed in the theoretical model as a semi-infinite medium is well justified.

For the case of elastic sea-beds, the code was modified to include shear wave effects in the medium. In this context, the eigenvalues and the corresponding eigenfunctions are complex. The eigenvalues are calculated using an impedance condition in the water-bottom interface [18] and the notion of the effective depth [19]. The use of the modified code (SHEAR) is for the time being restricted to homogeneous media (water and sea-bed) as it is the case in the experiments.

3.2. The parabolic approximation

As already stated, the experiments described in this paper are considered first steps towards the simulation of 3-D inverse procedures. Therefore it is essential that theoretical models to be used in both the forward and inverse propagation problems be also used in the calibration phase. For reasons related to the speed of the calculations, which is an essential factor in inverse procedures, 3-D codes based on parabolic approximation theory are considered as the main vehicle to predict the acoustic field in three dimensions. These codes are used here in the simple case of a range independent environment for consistency reasons with respect to the more complicated 3-D cases, where these codes would anyway be used.

The two numerical codes, which have been used for the calculation of the acoustic field using parabolic approximation theory, are briefly described here. Both codes were used to solve the acoustic problem for a point source emitting at a single frequency denoted f. The first code, 3DWAPE [20, 21] is an acoustic PE code, *i.e.* it assumes a multilayered fluid waveguide and hence does not handle shear waves in the sediment. Removing the cylindrical spreading factor $1/\sqrt{r}$ from the acoustic pressure p, it solves the following one-way equation

$$\frac{\partial p}{\partial r} = \mathrm{i}k_0 \sqrt{I + \frac{1}{k_0^2}\left[\rho \frac{\partial}{\partial z}\left(\frac{1}{\rho}\frac{\partial}{\partial z}\right) + \left(k^2 - k_0^2\right)\right]} p(r, z), \tag{4}$$

where I is identity, ρ is the density, $k_0 = \omega/c_0$ with c_0 a reference sound speed, and $k = (\omega/c)(1 + \mathrm{i}\eta\alpha_p)$ with c_p and α_p the compressional velocity and attenuation respectively, and $\eta = 1/(40\pi \log e)$. Parameters ρ, c_p and α_p are defined by their restrictions on each fluid layer ($p = \{w, b\}$). The square root operator present in the right-hand side of (4) is then approximated using a Padé series expansion. It should be noted that 3DWAPE is a full three-dimensional PE code (*i.e.*, it can handle horizontal refraction of the propagating field). Due to the experimental configuration, no coupling in the (crossing) azimuthal direction is expected. For the present study, a 2-D version of the code was thus run.

The second PE code is the seismo-acoustic PE code RAMS [22]. Removing the cylindrical spreading factor $1/\sqrt{r}$ from both the dilatation $\Delta = \Delta(r, z)$ and the vertical displacement $w = w(r, z)$, it solves the one-way equation

$$\frac{\partial}{\partial r}\begin{pmatrix} \Delta(r, z) \\ w(r, z) \end{pmatrix} = \mathrm{i}k_0 \sqrt{I + \frac{1}{k_0^2}\left(L^{-1}M - k_0^2 I\right)} \begin{pmatrix} \Delta(r, z) \\ w(r, z) \end{pmatrix}, \tag{5}$$

where the two matrices L and M contain the depth operators and depend on the Lamé constants $\lambda = \rho(\tilde{c}_p^2 - 2\tilde{c}_s^2)$ and $\mu = \rho\tilde{c}_s^2$, where $\tilde{c}_p = c_p/(1 + \mathrm{i}\eta\alpha_p)$ and $\tilde{c}_s = c_s/(1 + \mathrm{i}\eta\alpha_s)$ with c_p and c_s the real-valued compressional and shear velocities. The shear parameters are assumed to be null in

the water column. Equation (5) is then solved numerically using a split-step Padé algorithm [23].

4. Comparison of measurements with theoretical predictions

Several experiments were performed at LMA at different time periods under different environmental situations in order to check the repeatability of the experimental procedure using different configurations. Some characteristic test cases are presented here. The corresponding environmental parameters appear in Table I.

It should be noted that these parameters were measured either in situ or in previously performed experiments as explained in section 2.2. The measurements performed for some of these parameters were considered accurate and taking into account in addition that for some of them their influence in the calculation of the transmission loss is limited, they were considered constant and their average value was used in the calculations. These parameters were the sound speed in the water column c_w, (measured continuously through the temperature of the water) the density of the water and the sand ρ_w and ρ_b respectively and the positions of the source and receiver. A typical value of the attenuation coefficient in the sediment was considered, based on reported values for the type of sand used in the experiments.

The remaining two parameters, namely the sound speed of the sand c_b and the water depth h, both having major contribution in the acoustic field could not be considered known although for both of them, a priori estimations were given based on measurements described in section 2. Having obtained the acoustic field from direct measurements in the tank, a simple optimization procedure was initiated, and the values finally adopted for the comparisons, were based on the best match between predicted and measured values of the transmission loss. To this end, a search space for each one of the parameters indicated by the limits shown in table I was considered and a grid of possible values was formed. The theoretical models were used in connection with each point in the grid to predict the transmission loss. The TL calculated by the theoretical models was then compared to the experimental TL. The cost function used for the comparison was the error between the data points defined as

$$Rms = \sqrt{\sum_{i=1}^{n}(d_i - v_i)^2} \Big/ \sqrt{n},$$

where d is the experimental data, v_i the theoretical values and n is the number of data points. The data points are defined at each range step. Taking into account that near field estimations of the acoustic field are not considered accurate, while at the same time, near field measurements are not considered reliable, it has been decided that values in the beginning of data vector (corresponding to a range of 20 cm) were excluded from the optimization process.

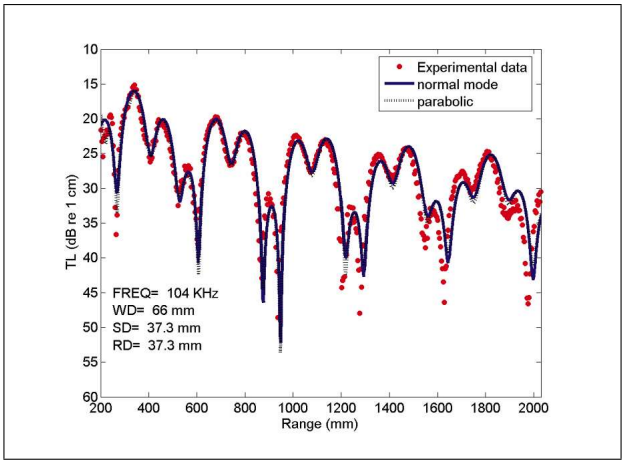

Figure 8. Test case 1: Comparison between theoretical and experimental data.

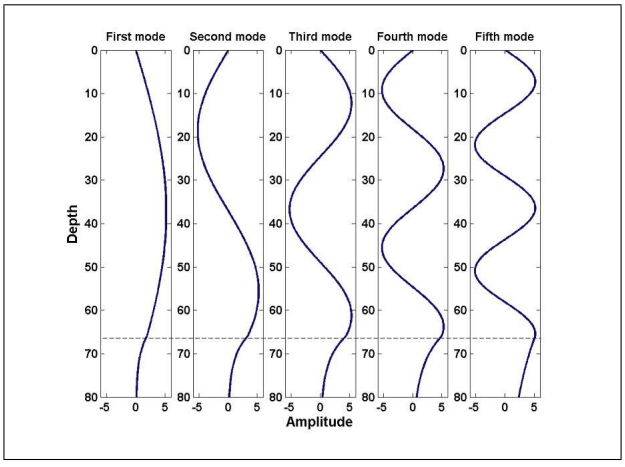

Figure 9. Test case 1: The five propagating modes (The bottom is indicated by a dashed line at 66 mm.

4.1. Test case 1

The water depth was determined using the procedure described in section 3.2 while the water temperature was 25.1 °C corresponding to a sound speed of 1496 m/s [15]. The source depth was kept constant and several measurements of the acoustic field were made in range and depth.

Figure 8 presents the transmission loss versus range for a typical configuration corresponding to a receiver depth of 37.3 mm, (the same as the source depth) and source frequency of 104 kHz. The minimum RMS error between measured and theoretical results was calculated to be 2.8 dB corresponding to $c_b = 1740$ m/s and $h = 66$ mm. The values in Figure 8 are based on a) the measured acoustic field, b) the normal-mode code MODE4 for fluid sediments and c) the parabolic equation based code 3DWAPE also for fluid sediments and appear in the figure as dots, solid, and dashed lines respectively. Since normal mode and parabolic approximation give almost identical results in the far field in the following tests and figures only the normal mode calculations will be presented.

Table I. The environmental parameters for the test cases. SD: Source depth, RD: Receiver depth, R: Range.

	TEST 1	TEST 2a	TEST 2b
c_w (m/s)	1496 (±0.5)	1478 (±0.5)	1478 (±0.5)
ρ_w (kg/m)	1000	1000	1000
h (mm)	66 (±0.5)	40 (±0.5)	40(±0.5)
c_b (m/s)	1700 (± 50)	1700(± 50)	1700(± 50)
ρ_b (kg/m)	1990 (±10)	1990 (±10)	1990 (±10)
α_b (dB/λ)	0.5 (±0.1)	0.5 (±0.1)	0.5 (±0.1)
SD (mm)	37.3 (±0.5)	10 (±0.5)	10 (±0.5)
RD (mm)	37.3 (±0.5)	17 (±0.5)	37(±0.5)
R (m)	0.3–2.3 (±0.2 cm)	0.25–3.1 (±0.2 cm)	0.25–3.1 (±0.2 cm)
f (kHz)	104	80	80

For the frequency of 104 kHz, 5 propagating modes are present in the waveguide. Therefore, a multi-mode structure of the sound speed is expected and it is actually illustrated in the figure. The 5 propagating modes appear in Figure 9. Note that due to the source and receiver depth (37.3 mm) modes 2 and 4 are weakly excited. The interference patterns observed in Figure 8 thus correspond to the contribution of only the other three propagating modes.

It is easily seen that a relatively good comparison between measured and simulated results do exist and the specific multi-mode structure is well represented. In fact for distances up to 1500 mm differences between experimental and theoretical data of less than 1 dB were observed with the exception of the locally extreme values. Nevertheless, for larger distances a discrepancy of more than 2 dB is observed at certain points. This discrepancy can be attributed to several factors one of which could be the shear excitation in the sandy substrate. It was thus decided to investigate the influence of shear excitation in the sediment in the acoustic field. Running the theoretical models including shear excitation in the bottom (codes SHEAR and RAMS), using the previously calculated parameters and varying only the shear speed between 0 and 400 m/s (with a step of 50 m/s) it was observed that the minimum RMS error was obtained for a shear speed of 300 m/s. Its value was 1.17 dB which is less than the corresponding RMS error of the previous calculations. The corresponding transmission loss versus range for the same configuration as in Figure 8, is presented in Figure 10. However, a shear speed of 300 m/s is certainly too high for this type of sediment and it is evident that in addition to the excitation of shear waves in the sand other factors are responsible for the discrepancy between experimental and theoretical results. For instance due to the finite geometry of the tank and the uncertainty about the efficiency of the absorbers used, the fundamental hypothesis of axisymetric environment is in doubt.

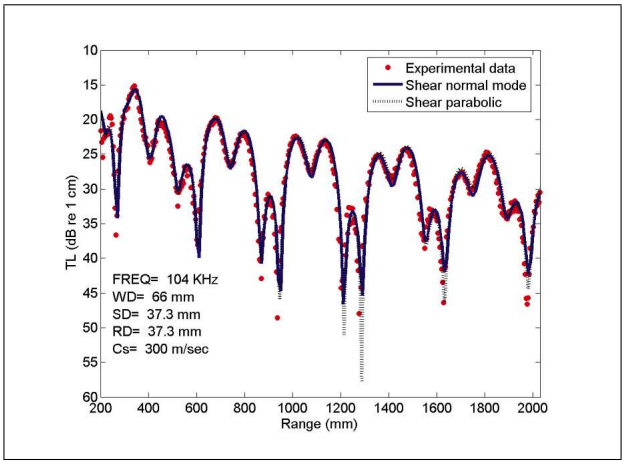

Figure 10. Test case 1: Comparison between theoretical and experimental data.

4.2. Test case 2

A second series of experiments were performed several weeks later, and were based on a configuration with different water depth and frequency (water depth about 40 mm and frequency 80 kHz). The bottom was the same. The purpose of these experiments was to confirm the repeatability of the experimental process as well as the values for the sediment layer used in the first series. In the environment of the second configuration, there were two propagating modes. The water temperature measured during the experiments corresponded to a sound speed in the water of 1478 m/s.

The results presented here correspond to two different receiver depths. First the receiver was put at the depth of 17 mm (Case 2a) and as a second configuration at the depth of 37 mm (Case 2b). The second receiver was intentionally put close to the bottom to study how the sediment layer in the tank affects the measurements made by a finite length transducer. Figure 11 presents the comparison between theoretical predictions and measured data for source depth equal to 10 mm, when no shear excitation is considered at the bottom. The minimum RMS error in this case was observed for $c_b = 1740$ m/s and $h = 40.1$ mm. The progressive shift between theoretical and experimental data is also present in this case and it is more pronounced with respect to Case 1. By assuming a shear speed of $c_s = 300$ m/s as in Case 1, we observe a better fit between theoretical and experimental data (Figure 12).

Similar observations are derived for Test Case 2b the results of which are presented in Figures 13 (fluid bottom)

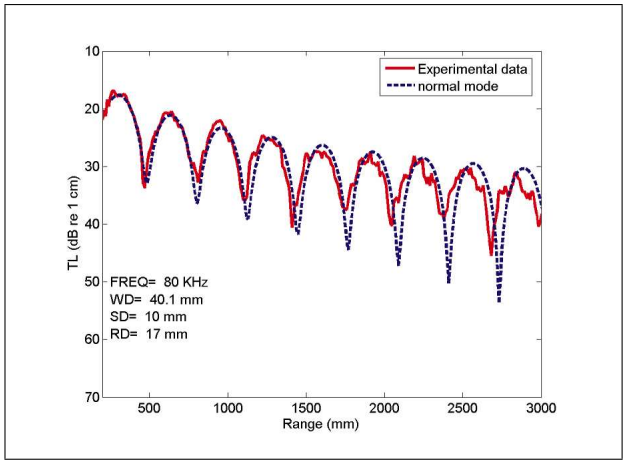

Figure 11. Test case 2a: Comparison between theoretical and experimental data.

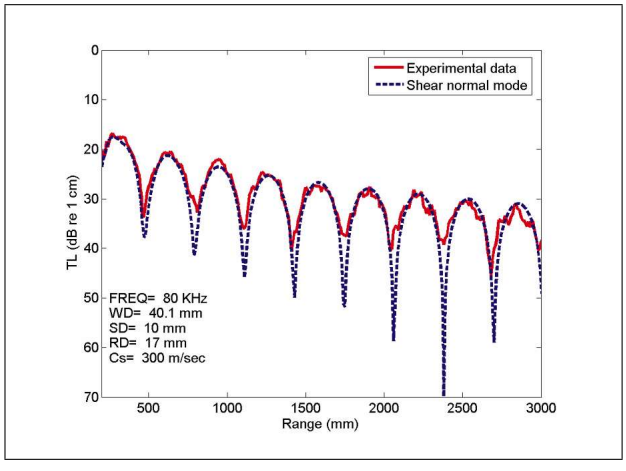

Figure 12. Test case 2a: Comparison between theoretical and experimental data.

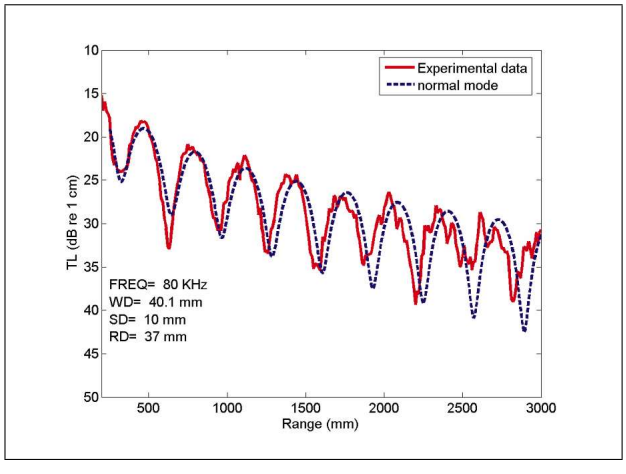

Figure 13. Test case 2b: Comparison between theoretical and experimental data.

and 14 (elastic bottom). Recall that the receiver is closer to the water bed in this case. The agreement between theoretical and experimental data in this case can not be considered as satisfactory as in large distances the corresponding

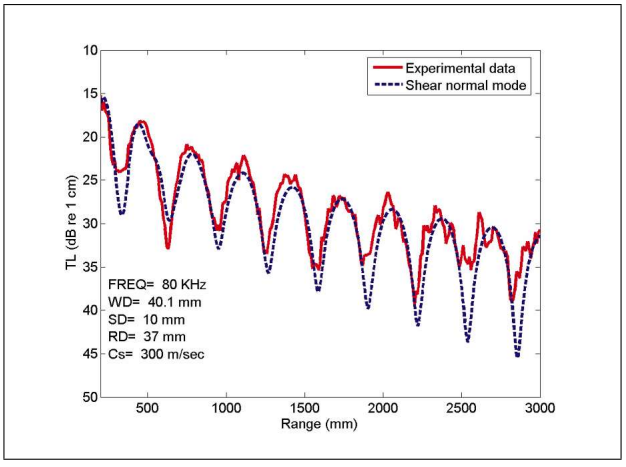

Figure 14. Test case 2b: Comparison between theoretical and experimental data.

differences exceed 5 dB. This can be attributed to the position of the receiver close to the bottom where the energy is relatively low. It is also reasonable to assume that in general the measurements are affected by the size of the transducer and therefore a perfect fit was not expected. This subject however needs further investigation.

5. Discussion

Tank experiments were performed aiming at the definition of calibration and experimental procedures appropriate to simulate real underwater acoustic propagation experiments and study inversion procedures associated with tomographic and geoacoustic inversion applications. A basic restriction of the tank experiments was that off-the-shelf equipment was to be used and the calibration procedures should be accordingly adapted. As a first step, range independent environments were considered and the reliability of the experimental procedures was checked by applying forward propagation models and comparing measurements of the acoustic field with theoretical predictions. Special care was taken to direct measure with the best possible accuracy the most sensitive acoustic parameters such as the sound speed in the water, and bottom as well as the water depth. Note that the authors have already undertaken the task to estimate these parameters from a wide search space, using optimization techniques, applicable in cases when accurate measurements of these parameters is not possible. The results of this study will be presented in future publication.

The experiments were conducted with success. The modal character of the acoustic field was easily observed and verified, as variations in range of the measured acoustic field expressed in terms of transmission loss, fit very well with associated variations of the calculated field based on normal-mode and parabolic approximation theory. In all the cases studied, in order to achieve better agreement between measured and predicted transmission loss, elastic properties were considered in the bottom. The

shear speed associated with the simulated sea-bed was indirectly determined using an optimization approach on the basis of the measured acoustic field but it came out to be higher than expected for this type of water saturated sand.

The conclusions from the present study can be summarized in the statement that the experimental set-up and the calibration scenarios adopted in the series of experiments described in this work can in principle be used in any type of scaled forward and inverse propagation experiments. Slight modifications of the calibration procedures could be necessary when more complicated situations are encountered. An additional objective will be to improve precision in the measurements of all the parameters of the experiment.

The tests to be performed in the future will focus on wave propagation in range-dependent environments by using appropriate material to simulate the geometry of the seafloor. Study of broad-band propagation and the analysis of the acoustic field in the time domain is underway, thus providing room for tank simulations of tomographic applications. Careful selection of the transducers is expected to enhance the agreement between measured and calculated fields, thus providing the necessary conditions for the creation of a data base of benchmark tank experiments aiming at the validation of inversion procedures in range independent and range dependent conditions, which is the ultimate goal of the authors.

Acknowledgement

This work has been partially supported by the Greek-French Co-operation Programme 2003-2006. The authors would like to express their sincere thanks to the associate editor and the anonymous reviewers for their constructive comments, which helped them to prepare the final version of the paper

References

[1] C. Gazanhes, J. P. Sessarego, J. L. Garnier: Identification of modes in some conditions of sound propagation in shallow water. J. Sound Vib **56** (1978) 251–259.

[2] C. T. Tindle, H. Hobaek, T. G. Muir: Downslope propagation of normal modes in a shallow water wedge. J. Acoust. Soc. Am. **81** (1987) 275–286.

[3] C. T. Tindle, H. Hobaek, T. G. Muir: Normal mode filtering for downslope propagation in a shallow water wedge. J. Acoust. Soc. Am. **81** (1987) 287–294.

[4] H. Hobaek, E. K. Westwood: Measurements of upslope wave-front curvature in a sand-bottom wedge. J. Acoust. Soc. Am. **84** (1988) 1787–1790.

[5] J. R. Chamuel, G. H. Brooke: Shallow water acoustic studies using an air-suspended water waveguide model. J. Acoust. Soc. Am. **84** (1988) 1777–1786.

[6] P. Cristini, J. L. Garnier, C. Gazanhes: Normal modes identification in shallow water using spectral anlysis: Theory and experiments. – In: Shear Waves in Marine Sediments. J. M. Hovem et al. (eds.). Kluwer, The Netherlands, 1991, 503–509.

[7] S. A. L. Glegg, A. J. Hundley, J. M. Riley, J. Yuan, H. Überall: Laboratory scale measurements and numerical predictions of underwater sound propagation over a sediment layer. J. Acoust. Soc. Am. **92** (1992) 1624–1630.

[8] S. Glegg, G. Deane, I. House: Comparison between theory and model scale measurements of 3d sound propagation in shear supporting penetrable wedge. J. Acoust. Soc. Am. **94** (1993) 2334–2342.

[9] M. Ainslie, L. Wabg, C. H. Harrison, N. G. Pace: Numerical and laboratory modelling of propagation over troughs and ridges. J. Acoust. Soc. Am. **94** (1993) 2287–2295.

[10] L. Wang, N. G. Pace, C. H. Harrison, M. Ainslie: Experimental study of sound propagation in modelled shallow water environments. Ultrasonics **32** (1994) 141–147.

[11] P. Cristini, F. Jensen, D. Morisset, J. Piraux, J. P. Sessarego: Experimental benchmarks for numerical propagation models: Comparison between numerical results and tank experiments for deep and shallow water environments. – In: ICTCA '97. Teng et al. (eds.). World Scientic Publishers, 1998, 667–678.

[12] J.-P. Sessarego: Scaled models for underwater acoustics and geotechnics applications. Proceedings of the Sixth European Conference on Underwater Acoustics, Gdansk, 2002, 359–366.

[13] P. Papadakis, M. Taroudakis, P. Sanchez, J.-P. Sessarego: Scaled laboratory experiments of shallow water acoustic propagation. Proceedings of Forum Acusticum 2005, Budapest, 2005, 287–292.

[14] F. Sturm, J.-P. Sessarego, P. Sanchez: Comparison of parabolic equation based codes with tank experiments for shallow water environments. Proceedings of the 8th European Conference on Underwater Acoustics 2006, Carvoeiro, 2006, Vol 1, 427–432.

[15] N. Bilaniuk, G. S. K. Wong: Speed of sound in pure water as a function of temperature. J. Acoust. Soc. Am. **93** (1609-1612) 1996.

[16] M. I. Taroudakis, G. A. Athanassoulis, J. P. Ioannidis: A hybrid solution of the Helmholtz equation in shallow water, based on a variational principle. Acoustique Sous Marine et Ultrasons, CNRS-LMA, Marseille, 1991, 213–227.

[17] F. B. Jensen et al.: Computational ocean acoustics. AIP Press, New York, 1994.

[18] M. I. Taroudakis, G. Makrakis: A study of the eigenvalues of the 'Depth Problemï in shallow water acoustic propagation modelling over an elastic halfspace. Proceedings of the 10th International Congress on Sound and Vibration, 2003, 2547–2553.

[19] Z. Y. Zhang, C. T. Tindle: Complex effective depth of ocean bottom. J. Acoust. Soc. Am. **93** (1993) 205–213.

[20] F. Sturm: Numerical study of broadband sound pulse propagation in three-dimensional oceanic waveguides. J. Acoust. Soc. Am. **117** (2005) 1058–1079.

[21] F. Sturm: Numerical simulations with 3DWAPE considering shallow water range-dependent environments. J. Acoust. Soc. Am. **109** (2001) 2aAOa13.

[22] M. D. Collins: Higher order Padé approximations for accurate and stable elastic parabolic equations with application to interface wave propagation. J. Acoust. Soc. Am. **89** (1991) 1050–1057.

[23] M. D. Collins: The split-step Padé solution for the parabolic equation method. J. Acoust. Soc. Am. **93** (1993) 1736–1742.